SCIENCE CHINA
Information Sciences

• RESEARCH PAPER •
Special Focus on 5G Wireless Communication Networks

February 2016, Vol. 59 022302:1–022302:14
doi: 10.1007/s11432-015-5509-1

Impact of RF mismatches on the performance of massive MIMO systems with ZF precoding

Hao WEI[1], Dongming WANG[1*], Jiangzhou WANG[2] & Xiaohu YOU[1]

[1]*National Mobile Communications Research Laboratory, Southeast University, Nanjing* 210096*, China;*
[2]*School of Engineering and Digital Arts, University of Kent, Canterbury* CT2 7NZ*, United Kingdom*

Received July 28, 2015; accepted November 24, 2015; published online January 4, 2016

Abstract Thanks to the channel reciprocity, the time division duplex (TDD) operation is more preferred in massive multiple-input multiple-output (MIMO) systems. Avoiding the heavy feedback of downlink channel state information (CSI) from the user equipment (UE) to the base station (BS), the uplink CSI can be exploited for the downlink precoding. However, due to the mismatches of the radio frequency (RF) circuits at both sides of the link, the whole communication channels are usually not symmetric in practical systems. This paper is focused on the RF mismatches at the UEs and the BS for the multi-user massive MIMO systems with zero forcing (ZF) precoding. The closed-form expressions of the ergodic sum-rates are derived for evaluating the impact of RF mismatches on the system performance. Theoretical analysis and simulation results show that the RF mismatches at the UEs only lead to a negligible performance loss. However, it is imperative to perform reciprocity calibration at the BS, because the RF mismatches at the BS contribute to the inter-user interference (IUI) and result in a severe system performance degradation.

Keywords massive MIMO, RF mismatch, TDD operation, channel reciprocity, antenna calibration

Citation Wei H, Wang D M, Wang J Z, et al. Impact of RF mismatches on the performance of massive MIMO systems with ZF precoding. Sci China Inf Sci, 2016, 59(2): 022302, doi: 10.1007/s11432-015-5509-1

1 Introduction

Multiple-input multiple-output (MIMO) antenna systems has been used in wireless communications to provide diversity gain and spatial multiplexing gain [1]. Scaling up MIMO to a large scale, classified as massive MIMO [2], potentially offers higher network capacity and better reliability. Therefore, massive MIMO has become a promising technique for the next generation wireless communication systems [3,4].

In a massive MIMO system, with the knowledge of the downlink channel state information (CSI) [5–7], the base station (BS) can use the precoding to simultaneously serve many user equipments (UE) in the same time-frequency resource [8]. However, for frequency division duplex (FDD) systems, the numbers of both the downlink pilots and the channel responses each UE must estimate are proportional to the number of antennas at the BS [3]. Thus, the overhead of the downlink pilots and the feedback of downlink

* Corresponding author (email: wangdm@seu.edu.cn)

CSI are much heavy and becomes unacceptable due to the large number of BS's antennas. While for time division duplex (TDD) operation, transmission signals experience the same physical perturbations in both uplink and downlink directions if the time interval is less than the channel coherence time [9]. Thanks to the channel reciprocity, the BS can obtain the CSI for both uplink and downlink channels through uplink pilots from the UEs. Therefore, TDD operation is more preferred for massive MIMO systems. Furthermore, the BS can use the zero forcing (ZF) precoding to transmit signals by exploiting the estimated CSI because of its high spectral efficiency [10].

However, in practical systems, the whole communication channel consists of not only the wireless propagation part, but also the transceiver radio frequency (RF) circuits at both sides of the link [11]. Normally, RF circuits include mixers, filters, analog to digital (A/D) converters, power amplifiers, etc., and are highly related to the temperature and humidity of the environment [12]. Although the wireless propagation channel is reciprocal, the mismatches of the transceiver RF circuits destroy the reciprocity of the whole communication channel. Hence, RF mismatches lead to a severe performance degradation of the system by damaging the ZF precoding and introducing the inter-user interference (IUI) [13]. Therefore, reciprocity calibration is necessary to maintain the channel symmetry for TDD systems.

To overcome the RF mismatches at both sides of link, total least squares based calibration was proposed for MIMO systems [12,14]. However, this method is based on exchanging the calibration signals between the transmitter and the receiver, of which the heavy feedback cannot be tolerated for massive MIMO systems. Thus, it is important to address how and how much the RF mismatches affect the system performance, in order to find more feasible calibration methods. There are many researches to study the RF mismatches. On the one hand, hardware calibration should be performed at both the BS and the UE for fully exploiting channel reciprocity [15,16]. On the other hand, Refs. [13] and [17] gave the conclusion that it is necessary to only perform calibration at the BS, and there is no need for calibration at the UE because the RF mismatches at the UE have little impact on system performance. Nevertheless, the impact of RF mismatches studied so far has been evaluated only by simulations. Therefore, it is essential to perform the theoretical analysis, which is the focus of our paper.

This paper is focused on the RF mismatches at the UEs and the BS respectively for the multi-user massive MIMO systems with ZF precoding. The analytical method can also be applied to large-scale distributed antenna systems (DASs) [18,19]. The main contributions of this paper include: Firstly, the amplitude and phase mismatches of RF gain at the UEs are investigated. The closed-form expressions for the lower bound of ergodic sum-rates are derived to evaluate the impact of RF mismatches on the system performance. Secondly, the amplitude and phase mismatches of RF gain at the BS are investigated. The closed-form expressions for the approximation of ergodic sum-rates are derived to evaluate the impact of RF mismatches on the system performance. Thirdly, according to theoretical analysis and simulation results, the RF mismatches at the UEs only lead to a negligible performance loss and there is no need to perform calibration at the UEs. However, it is imperative to perform reciprocity calibration at the BS, because the RF mismatches at the BS contribute to the IUI and result in a severe system performance degradation.

The rest of this paper is organized as follows. The general model of the RF gain for multi-user massive MIMO systems is described in Section 2. The impact of both the amplitude and phase mismatches at the UE on the system performance is studied in Section 3. In Section 4, the downlink sum-rates of the system considering both the amplitude and phase mismatches at the BS are investigated. Then, simulation results and discussions are presented in Section 5. Finally, conclusions are summarized in Section 6.

The notation adopted in this paper conforms to the following convention. Vectors are denoted in lower case bold: $\boldsymbol{x}$. Matrices are upper case bold: $\boldsymbol{A}$. $\boldsymbol{I}_M$ denotes the identity matrix of $M \times M$. $(\cdot)^*$, $(\cdot)^{\mathrm{T}}$ and $(\cdot)^{\mathrm{H}}$ represent conjugate, transpose, and Hermitian transpose, respectively. $\mathrm{Tr}(\boldsymbol{A})$ is the trace of $\boldsymbol{A}$. $[\boldsymbol{A}]_{ij}$ denotes the ith row jth column element of $\boldsymbol{A}$. The operator $\mathcal{E}(\cdot)$ denotes expectation. $\mathcal{N}(\mu, \sigma^2)$ stands for normal distribution with mean μ and variance σ^2. $\mathcal{U}[a, b]$ stands for uniform distribution on the interval $[a, b]$.

2 System model and fundamentals

In this section, a multi-user massive MIMO system with ZF precoding is considered. The BS is equipped with M antennas, and there are K single-antenna UEs in the system. $M \gg K$ is assumed for the massive MIMO system. The system model of RF mismatches and the receiving signals for the downlink transmission are presented.

2.1 Amplitude and phase mismatches of transceiver RF circuits

In practice, the whole communication channel consists of not only the wireless propagation part, but also the transceiver RF circuits of antennas at both sides of the link. Each antenna of the BS and a UE has a transmit RF and a receive RF module. $\boldsymbol{C}_{\mathrm{BS,t}}$ and $\boldsymbol{C}_{\mathrm{BS,r}}$ denote the transmit and receive RF matrices of the BS, respectively. $\boldsymbol{C}_{\mathrm{UE,t}}$ and $\boldsymbol{C}_{\mathrm{UE,r}}$ denote the transmit and receive RF matrices of the UEs, respectively. All of these matrices are diagonal. Define

$$\boldsymbol{C}_{\mathrm{BS,t}} = \mathrm{diag}\left(t_{\mathrm{BS},1}, \ldots, t_{\mathrm{BS},m}, \ldots, t_{\mathrm{BS},M}\right), \tag{1}$$

$$\boldsymbol{C}_{\mathrm{BS,r}} = \mathrm{diag}\left(r_{\mathrm{BS},1}, \ldots, r_{\mathrm{BS},m}, \ldots, r_{\mathrm{BS},M}\right), \tag{2}$$

$$\boldsymbol{C}_{\mathrm{UE,t}} = \mathrm{diag}\left(t_{\mathrm{UE},1}, \ldots, t_{\mathrm{UE},k}, \ldots, t_{\mathrm{UE},K}\right), \tag{3}$$

$$\boldsymbol{C}_{\mathrm{UE,r}} = \mathrm{diag}\left(r_{\mathrm{UE},1}, \ldots, r_{\mathrm{UE},k}, \ldots, r_{\mathrm{UE},K}\right), \tag{4}$$

where $t_{\mathrm{BS},m}$, $r_{\mathrm{BS},m}$ $(m = 1, \ldots, M)$ and $t_{\mathrm{UE},k}$, $r_{\mathrm{UE},k}$ $(k = 1, \ldots, K)$ are the RF gains characterized as $t_{\mathrm{BS},m} = |t_{\mathrm{BS},m}|e^{\iota\phi^{\mathrm{t}}_{\mathrm{BS},m}}$, $r_{\mathrm{BS},m} = |r_{\mathrm{BS},m}|e^{\iota\phi^{\mathrm{r}}_{\mathrm{BS},m}}$, $t_{\mathrm{UE},k} = |t_{\mathrm{UE},k}|e^{\iota\phi^{\mathrm{t}}_{\mathrm{UE},k}}$, $r_{\mathrm{UE},k} = |r_{\mathrm{UE},k}|e^{\iota\phi^{\mathrm{r}}_{\mathrm{UE},k}}$. The amplitudes of the RF gains are assumed to be of log-normal distribution [13,15], and the phases are assumed to be of uniform distribution [13,15,20]. Therefore, we have the following notations: $\ln|t_{\mathrm{BS},m}| \sim \mathcal{N}(0, \delta^2_{\mathrm{BS,t}})$, $\phi^{\mathrm{t}}_{\mathrm{BS},m} \sim \mathcal{U}[-\theta^{\mathrm{BS}}_{\mathrm{t}}, \theta^{\mathrm{BS}}_{\mathrm{t}}]$; $\ln|r_{\mathrm{BS},m}| \sim \mathcal{N}(0, \delta^2_{\mathrm{BS,r}})$, $\phi^{\mathrm{r}}_{\mathrm{BS},m} \sim \mathcal{U}[-\theta^{\mathrm{BS}}_{\mathrm{r}}, \theta^{\mathrm{BS}}_{\mathrm{r}}]$; $\ln|t_{\mathrm{UE},k}| \sim \mathcal{N}(0, \delta^2_{\mathrm{UE,t}})$, $\phi^{\mathrm{t}}_{\mathrm{UE},k} \sim \mathcal{U}[-\theta^{\mathrm{UE}}_{\mathrm{t}}, \theta^{\mathrm{UE}}_{\mathrm{t}}]$; $\ln|r_{\mathrm{UE},k}| \sim \mathcal{N}(0, \delta^2_{\mathrm{UE,r}})$, $\phi^{\mathrm{r}}_{\mathrm{UE},k} \sim \mathcal{U}[-\theta^{\mathrm{UE}}_{\mathrm{r}}, \theta^{\mathrm{UE}}_{\mathrm{r}}]$.

2.2 Downlink signal model

Considering the RF gains, the uplink and downlink channels are given by

$$\boldsymbol{G}_{\mathrm{UL}} = \boldsymbol{C}_{\mathrm{BS,r}}\boldsymbol{H}^{\mathrm{T}}\boldsymbol{C}_{\mathrm{UE,t}}, \tag{5}$$

$$\boldsymbol{G}_{\mathrm{DL}} = \boldsymbol{C}_{\mathrm{UE,r}}\boldsymbol{H}\boldsymbol{C}_{\mathrm{BS,t}}, \tag{6}$$

where $\boldsymbol{H} \in \mathbb{C}^{K\times M}$ represents the small-scale channel matrix, and each element $h_{km}(k = 1, \ldots, K; m = 1, \ldots, M)$ is a zero mean circularly symmetric complex Gaussian random variable of variance $1/2$ per dimension, which denotes the wireless channel coefficient from the mth antenna of the BS to the kth UE. From (5) and (6), the whole communication channel becomes non-reciprocal due to the RF mismatches, i.e. $\boldsymbol{G}_{\mathrm{DL}} \neq \boldsymbol{G}^{\mathrm{T}}_{\mathrm{UL}}$.

For clarity and brevity of analysis, uplink channel estimation is assumed ideal. Then, when ZF precoding is exploited by the BS, the overall downlink signals at the UEs are written as

$$\boldsymbol{y} = \beta\boldsymbol{G}_{\mathrm{DL}}\boldsymbol{G}^{*}_{\mathrm{UL}}\left(\boldsymbol{G}^{\mathrm{T}}_{\mathrm{UL}}\boldsymbol{G}^{*}_{\mathrm{UL}}\right)^{-1}\boldsymbol{x} + \boldsymbol{n}, \tag{7}$$

where $\beta = \sqrt{1/\mathrm{Tr}[(\boldsymbol{G}^{\mathrm{T}}_{\mathrm{UL}}\boldsymbol{G}^{*}_{\mathrm{UL}})^{-1}]}$ is the scaling factor to satisfy the transmit power constraint. $\boldsymbol{y} = [y_1, \ldots, y_K]^{\mathrm{T}}$ is the receiving signal vector. $\boldsymbol{x} = [x_1, \ldots, x_K]^{\mathrm{T}}$ is the signal vector transmitted to the UEs with the power constraint $\mathcal{E}[x_k x^*_k] = P$. $\boldsymbol{n}$ is the complex additive white Gaussian noise vector, in which the elements are independent and identically distributed (i.i.d.) complex Gaussian random variables with zero mean and variance σ^2_{n}.

Substituting (5) and (6) into (7), one obtains

$$\boldsymbol{y} = \beta\boldsymbol{C}_{\mathrm{UE,r}}\boldsymbol{W}\boldsymbol{C}^{-1}_{\mathrm{UE,t}}\boldsymbol{x} + \boldsymbol{n}, \tag{8}$$

where

$$\boldsymbol{W} = \left(\boldsymbol{H}\boldsymbol{C}_{\mathrm{BS,t}}\boldsymbol{C}_{\mathrm{BS,r}}^{*}\boldsymbol{H}^{\mathrm{H}}\right)\left(\boldsymbol{H}\boldsymbol{C}_{\mathrm{BS,r}}\boldsymbol{C}_{\mathrm{BS,r}}^{*}\boldsymbol{H}^{\mathrm{H}}\right)^{-1}. \tag{9}$$

Because of the RF mismatches at the BS, $\boldsymbol{C}_{\mathrm{BS,t}} \neq \boldsymbol{C}_{\mathrm{BS,r}}$, $\boldsymbol{W}$ is not equal to an identity matrix. Thus, the non-symmetric characteristic of the transceiver RF circuits will cause the IUI and degrade the system performance.

2.3 Ideal RF circuit

The case of ideal RF circuit is given for comparison, when there is no mismatch for RF gain. In the ideal case, RF gain matrices become identity matrices, which are given by

$$\boldsymbol{C}_{\mathrm{BS,t}}^{\mathrm{ideal}} = \boldsymbol{C}_{\mathrm{BS,r}}^{\mathrm{ideal}} = \boldsymbol{I}_{M}, \tag{10}$$

$$\boldsymbol{C}_{\mathrm{UE,t}}^{\mathrm{ideal}} = \boldsymbol{C}_{\mathrm{UE,r}}^{\mathrm{ideal}} = \boldsymbol{I}_{K}. \tag{11}$$

Then, the overall downlink receiving signals at the UEs are written as

$$\boldsymbol{y} = \beta_{\mathrm{ideal}}\boldsymbol{x} + \boldsymbol{n}, \tag{12}$$

$\beta_{\mathrm{ideal}} = \sqrt{1/\mathrm{Tr}[(\boldsymbol{H}\boldsymbol{H}^{\mathrm{H}})^{-1}]}$. When the number of antennas at BS is large, according to the characteristic of the Wishart matrices [21], we have

$$\mathrm{Tr}\left[\left(\boldsymbol{H}\boldsymbol{H}^{\mathrm{H}}\right)^{-1}\right] \xrightarrow{\text{a.s.}} \frac{K}{M-K}, \tag{13}$$

where "a.s." is the abbreviation of "almost sure". Thus, we obtain the signal-to-interference-plus-noise-ratio (SINR) of the ith UE as follows

$$\gamma_{i}^{\mathrm{ideal}} = \frac{P}{\sigma_{\mathrm{n}}^{2}} \cdot \beta_{\mathrm{ideal}}^{2} = \rho \cdot \frac{M-K}{K}, \tag{14}$$

where $\rho = P/\sigma_{\mathrm{n}}^{2}$. Then, the sum-rates of all UEs are given by

$$R^{\mathrm{ideal}} = \sum_{i=1}^{K} R_{i}^{\mathrm{ideal}} = \sum_{i=1}^{K} \log\left(1+\gamma_{i}^{\mathrm{ideal}}\right). \tag{15}$$

At high SNR, we further obtain the lower bound of the sum-rates [10]

$$R_{\mathrm{LB}}^{\mathrm{ideal}} = \sum_{i=1}^{K} \log\left(\gamma_{i}^{\mathrm{ideal}}\right) = K \cdot \left[\log\left(\rho\right) + \log\left(\frac{M-K}{K}\right)\right]. \tag{16}$$

3 Impact of RF mismatches at UE

For clarity of analysis, the impact of RF mismatches on the system performance at the UE and the BS are investigated separately.

Considering the amplitude and phase mismatches at the UEs, the uplink and downlink channel matrices are rewritten as

$$\boldsymbol{G}_{\mathrm{UL}} = \boldsymbol{H}^{\mathrm{T}}\boldsymbol{C}_{\mathrm{UE,t}}, \tag{17}$$

$$\boldsymbol{G}_{\mathrm{DL}} = \boldsymbol{C}_{\mathrm{UE,r}}\boldsymbol{H}. \tag{18}$$

Then, substituting (17) and (18) into (7), the downlink signals at the UEs are given by

$$\boldsymbol{y} = \beta_{\mathrm{UE\_mis}}\boldsymbol{C}_{\mathrm{UE,r}}\boldsymbol{C}_{\mathrm{UE,t}}^{-1}\boldsymbol{x} + \boldsymbol{n}, \tag{19}$$

where $\beta_{\mathrm{UE\_mis}} = \sqrt{1/\mathrm{Tr}[(\boldsymbol{C}_{\mathrm{UE,t}}\boldsymbol{H}\boldsymbol{H}^{\mathrm{H}}\boldsymbol{C}_{\mathrm{UE,t}}^{*})^{-1}]}$. From (19), we can see that the RF mismatches at the UE do not contribute to the IUI.

When the number of antennas at the BS is large, one obtains [21]

$$\mathrm{Tr}\left[\left(\boldsymbol{C}_{\mathrm{UE,t}}\boldsymbol{H}\boldsymbol{H}^{\mathrm{H}}\boldsymbol{C}^{*}_{\mathrm{UE,t}}\right)^{-1}\right] \xrightarrow{\text{a.s.}} \frac{1}{M-K}\cdot\sum_{i=1}^{K}\frac{1}{|t_{\mathrm{UE},i}|^2}. \tag{20}$$

Then, for large M, the SINR of the ith UE is given by

$$\gamma_i^{\mathrm{UE\_mis}} = \rho\cdot\beta^2_{\mathrm{UE\_mis}}\cdot\frac{|r_{\mathrm{UE},i}|^2}{|t_{\mathrm{UE},i}|^2}. \tag{21}$$

Therefore, the sum-rates of all UEs under the RF mismatches are given by

$$R^{\mathrm{UE\_mis}} = \sum_{i=1}^{K} R_i^{\mathrm{UE\_mis}} = \sum_{i=1}^{K}\log\left(1+\gamma_i^{\mathrm{UE\_mis}}\right). \tag{22}$$

Using (21), the ergodic rate of the ith UE is given by

$$\mathcal{E}\left[R_i^{\mathrm{UE\_mis}}\right] = \mathcal{E}\left[\log\left(1+\rho\cdot\beta^2_{\mathrm{UE\_mis}}\cdot\frac{|r_{\mathrm{UE},i}|^2}{|t_{\mathrm{UE},i}|^2}\right)\right]. \tag{23}$$

With the following Jensen's inequality [22,23]

$$\mathcal{E}\left[\log\left(1+e^{\ln x}\right)\right] \geqslant \log\left(1+e^{\mathcal{E}[\ln x]}\right),$$

we have

$$\begin{aligned}\mathcal{E}\left[R_i^{\mathrm{UE\_mis}}\right] &\geqslant \log\left\{1+\exp\left(\mathcal{E}\left[\ln\left(\rho\cdot\beta^2_{\mathrm{UE\_mis}}\cdot\frac{|r_{\mathrm{UE},k}|^2}{|t_{\mathrm{UE},i}|^2}\right)\right]\right)\right\}\\ &= \log\left\{1+\exp\left(\ln(\rho)+\ln(M-K)-\mathcal{E}\left[\ln\left(\sum_{i=1}^{K}\frac{1}{|t_{\mathrm{UE},i}|^2}\right)\right]\right)\right\}.\end{aligned} \tag{24}$$

Since $\ln(x)$ is a concave function, one obtains

$$\mathcal{E}\left[\ln\left(\sum_{i=1}^{K}\frac{1}{|t_{\mathrm{UE},i}|^2}\right)\right] \leqslant \ln\left[\mathcal{E}\left(\sum_{i=1}^{K}\frac{1}{|t_{\mathrm{UE},i}|^2}\right)\right] = \ln\left(K\cdot e^{2\delta^2_{\mathrm{UE,t}}}\right). \tag{25}$$

Substituting (25) into (24), a lower bound of the ergodic sum-rates is given by

$$\mathcal{E}\left[R^{\mathrm{UE\_mis}}\right]_{\mathrm{LB1}} = K\cdot\log\left\{1+\rho\cdot\frac{M-K}{K}\cdot e^{-2\delta^2_{\mathrm{UE,t}}}\right\}. \tag{26}$$

At high SNR, we further obtain another much lower bound of the ergodic sum-rates

$$\begin{aligned}\mathcal{E}\left[R^{\mathrm{UE\_mis}}\right]_{\mathrm{LB2}} &= K\cdot\left[\log\left(\rho\cdot\frac{M-K}{K}\cdot e^{-2\delta^2_{\mathrm{UE,t}}}\right)\right]\\ &= K\cdot\left[\log(\rho)+\log\left(\frac{M-K}{K}\right)-\left(\log e\cdot 2\delta^2_{\mathrm{UE,t}}\right)\right]\\ &= R^{\mathrm{ideal}}_{\mathrm{LB}}-\Delta R^{\mathrm{mis}}_{\mathrm{UE}},\end{aligned} \tag{27}$$

where

$$\Delta R^{\mathrm{mis}}_{\mathrm{UE}} = K\cdot\left\{\log e\cdot 2\delta^2_{\mathrm{UE,t}}\right\} \tag{28}$$

is the system performance loss due to the RF mismatches at the UEs. According to (28), the sum-rates decrease slightly if the variance of the amplitude mismatch is small, and the phase mismatch causes no degradation on the system throughput. It can be seen that the RF mismatches at the UEs can be handled by transmitting pilots through the precoding to the UEs. The overhead for these supplementary pilots is very small [3], which scales linearly with the number of the UEs.

4 Impact of RF mismatches at BS

Considering the amplitude and phase mismatches at the BS, the uplink and downlink channel matrices are rewritten as

$$\boldsymbol{G}_{\mathrm{UL}} = \boldsymbol{C}_{\mathrm{BS,r}}\boldsymbol{H}^{\mathrm{T}}, \tag{29}$$

$$\boldsymbol{G}_{\mathrm{DL}} = \boldsymbol{H}\boldsymbol{C}_{\mathrm{BS,t}}. \tag{30}$$

Then, substituting (29) and (30) into (7), the downlink signals at the UEs are given by

$$\boldsymbol{y} = \beta_{\mathrm{BS\_mis}}\boldsymbol{W}\boldsymbol{x} + \boldsymbol{n}, \tag{31}$$

where $\beta_{\mathrm{BS\_mis}} = \sqrt{1/\mathrm{Tr}[(\boldsymbol{H}\boldsymbol{C}_{\mathrm{BS,t}}\boldsymbol{C}^{*}_{\mathrm{BS,t}}\boldsymbol{H}^{\mathrm{H}})^{-1}]}$. Similar to (20), we have

$$\mathrm{Tr}\left[\left(\boldsymbol{H}\boldsymbol{C}_{\mathrm{BS,r}}\boldsymbol{C}^{*}_{\mathrm{BS,r}}\boldsymbol{H}^{\mathrm{H}}\right)^{-1}\right] \xrightarrow{\text{a.s.}} \frac{K}{M-K}\cdot\left(\frac{1}{M}\sum_{m=1}^{M}|r_{\mathrm{BS},m}|^{2}\right)^{-1}.$$

When the number of antennas at BS is large, e.g.

$$\lim_{M\to\infty}\frac{1}{M}\sum_{m=1}^{M}|r_{\mathrm{BS},m}|^{2} = e^{2\delta^{2}_{\mathrm{BS,r}}},$$

we obtain

$$\mathrm{Tr}\left[\left(\boldsymbol{H}\boldsymbol{C}_{\mathrm{BS,r}}\boldsymbol{C}^{*}_{\mathrm{BS,r}}\boldsymbol{H}^{\mathrm{H}}\right)^{-1}\right] \xrightarrow{\text{a.s.}} \frac{K}{M-K}\cdot e^{-2\delta^{2}_{\mathrm{BS,r}}}. \tag{32}$$

From (31), it can be seen that the non-reciprocity of the RF gain at the BS will result in the IUI. Hence, the receiving signal of the ith UE is

$$y_i = \beta_{\mathrm{BS\_mis}}[\boldsymbol{W}]_{ii}x_i + \beta_{\mathrm{BS\_mis}}\sum_{j=1,j\neq i}^{K}[\boldsymbol{W}]_{ij}x_j + n_i, \tag{33}$$

and the SINR of the ith UE is

$$\gamma_i^{\mathrm{BS\_mis}} = \frac{\rho\cdot\beta^{2}_{\mathrm{BS\_mis}}\cdot|[\boldsymbol{W}]_{ii}|^{2}}{\rho\cdot\beta^{2}_{\mathrm{BS\_mis}}\cdot\sum_{j=1,j\neq i}^{K}|[\boldsymbol{W}]_{ij}|^{2}+1}. \tag{34}$$

Then the sum-rates of all UEs under RF mismatches are

$$R^{\mathrm{BS\_mis}} = \sum_{i=1}^{K}R_i^{\mathrm{BS\_mis}} = \sum_{i=1}^{K}\log\left(1+\gamma_i^{\mathrm{BS\_mis}}\right). \tag{35}$$

In order to derive $[\boldsymbol{W}]_{ii}$, we introduce a variable $\tau_m = t_{\mathrm{BS},m}/r_{\mathrm{BS},m}$ $(m=1,\ldots,M)$ and define a matrix $\boldsymbol{H}^{\tau}_{ii}$ $(i=1,\ldots,K)\in\mathbb{C}^{K\times M}$ as

$$\boldsymbol{H}^{\tau}_{ii} = \begin{bmatrix} h_{11} & \cdots & h_{1m} & \cdots & h_{1M} \\ \vdots & & \vdots & & \vdots \\ h_{(i-1)1} & \cdots & h_{(i-1)m} & \cdots & h_{(i-1)M} \\ h_{i1}\tau_1 & \cdots & h_{im}\tau_m & \cdots & h_{iM}\tau_M \\ h_{(i+1)1} & \cdots & h_{(i+1)m} & \cdots & h_{(i+1)M} \\ \vdots & & \vdots & & \vdots \\ h_{K1} & \cdots & h_{Km} & \cdots & h_{KM} \end{bmatrix}. \tag{36}$$

Then, according to the characteristic of the matrix, we have

$$[\boldsymbol{W}]_{ii} = \frac{\det\left(\boldsymbol{H}^{\tau}_{ii}\boldsymbol{C}_{\mathrm{BS,r}}\boldsymbol{C}^{*}_{\mathrm{BS,r}}\boldsymbol{H}^{\mathrm{H}}\right)}{\det\left(\boldsymbol{H}\boldsymbol{C}_{\mathrm{BS,r}}\boldsymbol{C}^{*}_{\mathrm{BS,r}}\boldsymbol{H}^{\mathrm{H}}\right)}. \tag{37}$$

Theorem 1. From (37), when the number of BS antennas is large, i.e. $M \to \infty$, we can get the approximation as follows

$$|[\boldsymbol{W}]_{ii}|^2 = \frac{e^{\delta^2_{\mathrm{BS,t}}+\delta^2_{\mathrm{BS,r}}} \cdot \mathrm{sinc}^2\left(\theta_{\mathrm{BS,t}}\right) \cdot \mathrm{sinc}^2\left(\theta_{\mathrm{BS,r}}\right)}{e^{4\delta^2_{\mathrm{BS,r}}}}. \tag{38}$$

Proof. See Appendix A.

Consequently, in order to investigate $[\boldsymbol{W}]_{ij}$, we define a matrix $\boldsymbol{H}^{\tau}_{ij}\,(i,j=1,\ldots,K) \in \mathbb{C}^{K\times M}$ as

$$\boldsymbol{H}^{\tau}_{ij} = \begin{bmatrix} h_{11} & \cdots & h_{1m} & \cdots & h_{1M} \\ \vdots & & \vdots & & \vdots \\ h_{i1} & \cdots & h_{im} & \cdots & h_{iM} \\ \vdots & & \vdots & & \vdots \\ h_{(j-1)1} & \cdots & h_{(j-1)m} & \cdots & h_{(j-1)M} \\ h_{i1}\tau_1 & \cdots & h_{im}\tau_m & \cdots & h_{iM}\tau_M \\ h_{(j+1)1} & \cdots & h_{(j+1)m} & \cdots & h_{(j+1)M} \\ \vdots & & \vdots & & \vdots \\ h_{K1} & \cdots & h_{Km} & \cdots & h_{KM} \end{bmatrix}. \tag{39}$$

Then, according to the characteristic of the matrix determinant, we have

$$[\boldsymbol{W}]_{ij} = \frac{\det\left(\boldsymbol{H}^{\tau}_{ij}\boldsymbol{C}_{\mathrm{BS,r}}\boldsymbol{C}^{*}_{\mathrm{BS,r}}\boldsymbol{H}^{\mathrm{H}}\right)}{\det\left(\boldsymbol{H}\boldsymbol{C}_{\mathrm{BS,r}}\boldsymbol{C}^{*}_{\mathrm{BS,r}}\boldsymbol{H}^{\mathrm{H}}\right)}. \tag{40}$$

Theorem 2. From (40), when the number of BS antennas is large, i.e. $M \to \infty$, we can get the following approximation

$$\left|[\mathbf{W}]_{ij}\right|^2 = \frac{1}{M} \cdot \frac{1}{e^{2\delta^2_{\mathrm{BS,r}}}} \cdot \left[e^{2\delta^2_{\mathrm{BS,t}}} + e^{2\delta^2_{\mathrm{BS,r}}} - 2e^{\delta^2_{\mathrm{BS,t}}/2+\delta^2_{\mathrm{BS,r}}/2} \cdot \mathrm{sinc}\left(\theta_{\mathrm{BS,t}}\right) \cdot \mathrm{sinc}\left(\theta_{\mathrm{BS,r}}\right)\right]. \tag{41}$$

Proof. See Appendix B.

Then, the ergodic rate of the ith UE under RF mismatches of BS is given by

$$\mathcal{E}\left[R_i^{\mathrm{BS\_mis}}\right] = \log\left\{1 + \frac{\rho \cdot \frac{M-K}{K} \cdot \lambda_1}{\rho \cdot \frac{(K-1)(M-K)}{K\cdot M} \cdot \lambda_2 + 1}\right\}, \tag{42}$$

where

$$\begin{aligned} \lambda_1 &= \mathrm{sinc}^2\left(\theta_{\mathrm{BS,t}}\right) \cdot \mathrm{sinc}^2\left(\theta_{\mathrm{BS,r}}\right), \\ \lambda_2 &= e^{2\delta^2_{\mathrm{BS,t}}} + e^{2\delta^2_{\mathrm{BS,r}}} - 2e^{\delta^2_{\mathrm{BS,t}}/2+\delta^2_{\mathrm{BS,r}}/2} \cdot \mathrm{sinc}\left(\theta_{\mathrm{BS,t}}\right) \cdot \mathrm{sinc}\left(\theta_{\mathrm{BS,r}}\right). \end{aligned} \tag{43}$$

At high SNR, we further obtain the lower bound of the ergodic sum-rates

$$\mathcal{E}\left[R^{\mathrm{BS\_mis}}\right]_{\mathrm{LB}} = K \cdot \left\{\log\left(\frac{M}{K-1} \cdot \frac{\lambda_1}{\lambda_2}\right)\right\} = R^{\mathrm{ideal}}_{\mathrm{LB}} - \Delta R^{\mathrm{mis}}_{\mathrm{BS}}, \tag{44}$$

where

$$\Delta R^{\mathrm{mis}}_{\mathrm{BS}} = K \cdot \left\{\log\left(\rho\right) + \log\left(\frac{\lambda_2}{\lambda_1}\right) - \log\left[\frac{M \cdot K}{(M-K)\,(K-1)}\right]\right\} \tag{45}$$

is the performance loss due to the RF mismatches at the BS. It can be seen from (45) that the performance loss is not only related to the RF mismatches, but also increase with the transmit power. From the analysis

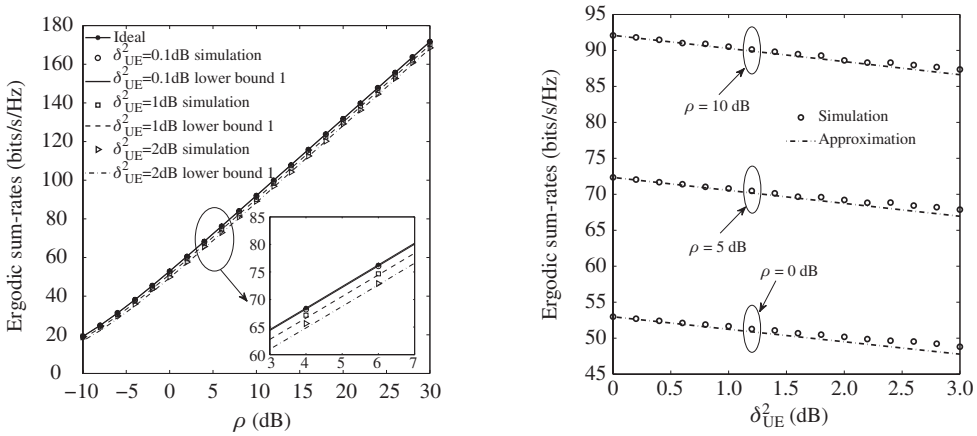

Figure 1 (a) Ergodic sum-rates versus the transmit power of the BS; (b) ergodic sum-rates versus the amplitude variance of RF mismatches $\delta^2_{\rm UE}$ at the UEs.

above, for BS, both amplitude and phase mismatches will result in a severe performance degradation. Hence, it is important and imperative to perform reciprocity calibration at the BS.

Fortunately, we can multiply the precoding matrix by a calibration diagonal matrix $\boldsymbol{C}_{\rm cal}$ on the left, which satisfies $\boldsymbol{C}_{\rm BS,t}\boldsymbol{C}_{\rm cal} = \alpha_{\rm cal}\boldsymbol{C}_{\rm BS,r}$. $\alpha_{\rm cal}$ is a non-zero scalar. It is dependent on the calibration method and has no impact on the system performance, since it can be eliminated by normalizing the transmitting power. Then, after the perfect calibration, the receiving signals at the UE can be written as

$$\boldsymbol{y} = \alpha_{\rm cal}\beta_{\rm cal}\boldsymbol{C}_{\rm UE,r}\boldsymbol{C}^{-1}_{\rm UE,t}\boldsymbol{x} + \boldsymbol{n}, \tag{46}$$

where $\beta_{\rm cal}$ is the scaling factor under calibration. With respect to (19), we can see that the IUI caused by the RF mismatches at the BS can be eliminated through the reciprocity calibration.

5 Simulation results

In this section, simulations are performed to show the impact of RF mismatches on the system performance and validate the theoretical analysis. The simulation parameters are set as follows. The number of antennas at the BS is 256, which serves 12 single-antenna UEs.

5.1 Impact of RF mismatches at the UE

Figure 1 illustrates the impact of the amplitude mismatches of the RF gain at the UEs. Let the amplitude variance of RF mismatches at the UEs $\delta^2_{\rm UE,t} = \delta^2_{\rm UE,r} = \delta^2_{\rm UE}$, and set $\delta^2_{\rm UE}$ be 0.1, 1, and 2 dB respectively. From Figure 1(a), it can be seen that all the ergodic sum-rates for different setups increase with ρ. That is, the amplitude mismatches cause no IUI on the system performance, which is consistent with (26). It is also shown that the curves are very close even though $\delta^2_{\rm UE}$ increases from 0.1 to 2 dB, so that the amplitude mismatches degrade the system performance very slightly. As shown in Figure 1(b), the performance loss is only about 5% when $\delta^2_{\rm UE}$ is 3 dB. Further, ergodic sum-rates decrease approximately linearly with the amplitude variance, which is consistent with the theoretical result (28).

Figure 2 demonstrates the impact of the phase mismatches of the RF gain at the UEs. Let the phase range of RF mismatches at the UE $\theta_{\rm UE,t} = \theta_{\rm UE,r} = \theta_{\rm UE}$, and set $\theta_{\rm UE}$ be $\pi/12$, $\pi/6$ and $\pi/3$ respectively. From Figure 2(a), it can be seen that all the ergodic sum-rates for different setups are the same, although their phase ranges $\theta_{\rm UE}$ are different. It is also seen from Figure 2(b) that ergodic sum-rates keep constant with the variance of $\theta_{\rm UE}$. Then, we can draw the conclusion that the phase mismatches of the RF gain at the UEs have no impact on the system performance.

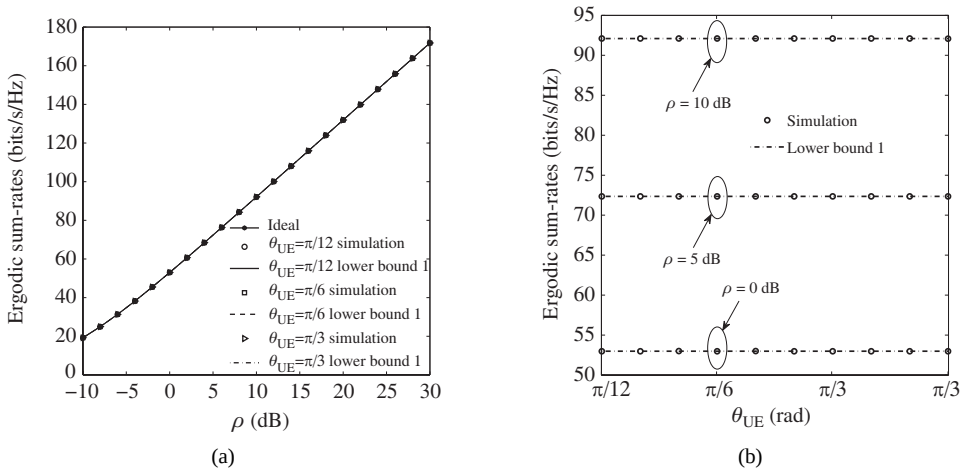

Figure 2 (a) Ergodic sum-rates versus the transmit power of the BS; (b) ergodic sum-rates versus the phase range of RF mismatches θ_{UE} at the UE.

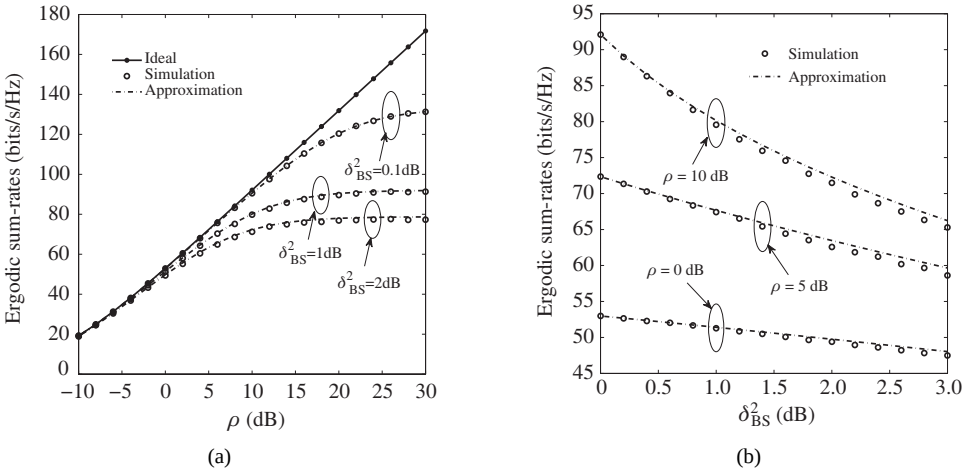

Figure 3 (a) Ergodic sum-rates versus the transmit power of the BS; (b) ergodic sum-rates versus the amplitude variance of RF gain mismatch δ^2_{BS} at the BS.

5.2 Impact of RF mismatches at the BS

Figure 3 depicts the impact of the amplitude mismatches of the RF gain at the BS. Let the amplitude variance of RF gain at the BS $\delta^2_{\mathrm{BS,t}} = \delta^2_{\mathrm{BS,r}} = \delta^2_{\mathrm{BS}}$, and set δ^2_{BS} be 0.1, 1, and 2 dB respectively. From Figure 3(a), it can be seen that ergodic sum-rates increase gradually with the transmit power, but approach a limit when ρ increases to the high region. In other words, the amplitude mismatches cause the IUI on the system performance, which is proved by (42) and (43). When δ^2_{BS} increases from 0.1 to 2 dB, the sum-rates decrease significantly because of the IUI. As shown in Figure 3(b), the larger ρ is, the severer the performance loss is, which is consistent with the theoretical result (45). When δ^2_{BS} is 3 dB and ρ is 10 dB, the performance loss is almost 30%.

Figure 4 demonstrates the impact of the phase mismatches of the RF gain at BS. Let the phase range of RF mismatches at the BS $\theta_{\mathrm{BS,t}} = \theta_{\mathrm{BS,r}} = \theta_{\mathrm{BS}}$, and set θ_{BS} be $\pi/12$, $\pi/6$ and $\pi/3$ respectively. From Figure 4(a), it can be seen that ergodic sum-rates increase gradually with the transmit power, but approach a limit when ρ increases to the high region. According to (42) and (43), the phase mismatches of the RF gain at BS not only cause the IUI, but also degrade the power of the signal transmitted to the intended user, both of which result in the great loss of the system performance. From Figure 4(b), it can also be seen that the higher the transmit power is, the more severely the ergodic sum-rates decrease, which is consistent with the theoretical result (45). When θ_{BS} is $\pi/3$ and ρ is 10 dB, the performance

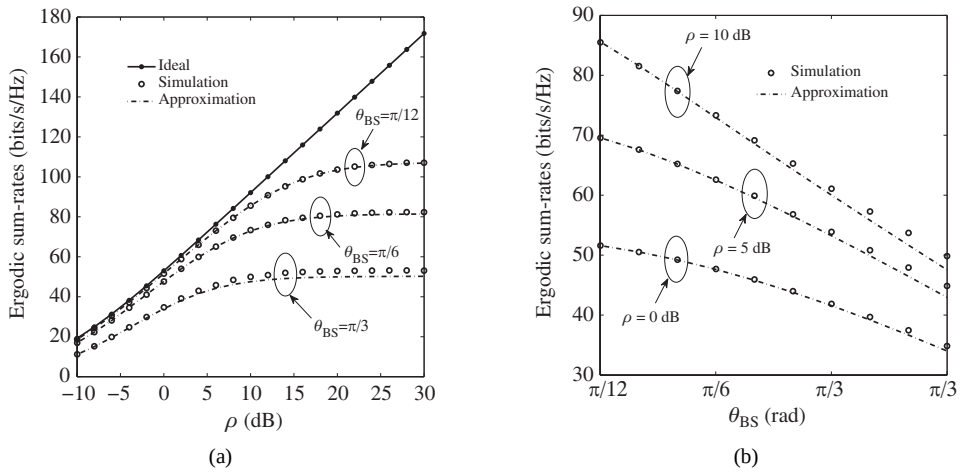

Figure 4 (a) Ergodic sum-rates versus the transmit power of the BS; (b) ergodic sum-rates versus the phase range of RF mismatches $\theta_{\rm BS}$ at the BS.

loss is almost 45%, which is unsatisfactory.

From the simulation results, we can draw the conclusion that the RF mismatches at the UEs only lead to a negligible performance loss. However, it is imperative to perform reciprocity calibration at the BS, because the RF mismatches at the BS contribute to the IUI and result in a severe system performance degradation. Therefore, compared with the method in [12,14], more feasible calibration methods were proposed in [24,25]. Only the antennas of the BS were involved to exchange the calibration signals. The UEs were excluded from the calibration procedure and the feedback was not required.

6 Conclusion

In this paper, we have carried out investigation in the impact of the RF mismatches on the performance of multi-user massive MIMO systems with ZF precoding. Due to the gain mismatches of the transceiver RF circuits, the whole communication channel is actually not reciprocal, and the uplink CSI cannot be simply used for performing the downlink precoding. According to our theoretical analysis and simulations, for the RF gain mismatches at the UEs, the phase mismatches cause no decrease on the system throughput, and only the amplitude mismatches lead to a slight performance loss. While the RF mismatches at the BS are the major factor of contributing to the IUI, both the amplitude and the phase mismatches result in a severe system performance degradation. Therefore, there is no need to calibrate the RF mismatches at the UE, but it is important and imperative to perform the reciprocity calibration at the BS.

Acknowledgements

This work was supported in part by National Basic Research Program of China (973 Program) (Grant Nos. 2013CB336600, 2012CB316004), National Natural Science Foundation of China (Grant Nos. 61221002, 61271205), National High-tech R&D Program of China (863 Program) (Grant No. 2014AA01A706), Colleges and Universities in Jiangsu Province Plans to Graduate Research and Innovation KYLX15_0075.

Conflict of interest The authors declare that they have no conflict of interest.

References

1 Zhu H L. Performance comparison between distributed antenna and microcellular systems. IEEE J Sel Area Commun, 2011, 29: 1151–1163

2 Rusek F, Persson D, Lau B K, et al. Scaling up MIMO: opportunities and challenges with very large arrays. IEEE Signal Process Mag, 2013, 30: 40–60

3 Erik L, Edfors O, Tufvesson F, et al. Massive MIMO for next generation wireless systems. IEEE Commun Mag, 2014, 2: 186–195
4 Ma Z, Zhang Z, Ding Z, et al. Key techniques for 5G wireless communications: network architecture, physical layer, and MAC layer perspectives. Sci China Inf Sci, 2015, 58: 041301
5 Zhu H L, Wang J Z. Chunk-based resource allocation in OFDMA systems—Part I: chunk allocation. IEEE Trans Wirel Commun, 2009, 57: 2734–2744
6 Zhu H L, Wang J Z. Chunk-based resource allocation in OFDMA systems—Part II: joint chunk, power and bit allocation. IEEE Trans Wirel Commun, 2012, 60: 499–509
7 Zhu H L. Radio resource allocation for OFDMA systems in high speed environments. IEEE J Sel Area Commun, 2012, 30: 748–759
8 Huh H, Caire Giuseppe, Papadopoulos H C, et al. Achieving massive MIMO spectral efficiency with a not-so-large number of antennas. IEEE Trans Wirel Commun, 2011, 11: 3226–3239
9 Smith G S. A direct derivation of a single-antenna reciprocity relation for the time domain. IEEE Trans Antenn Propag, 2004, 52: 1568–1577
10 Hong Y, Marzetta T L. Performance of conjugate and zero-forcing beamforming in large-scale antenna systems. IEEE J Sel Area Commun, 2013, 31: 172–179
11 Bourdoux A. Non-reciprocal transceivers in OFDM/SDMA systems: impact and mitigation. In: Proceedings of IEEE Radio and Wireless Conference (RAWCON 03), Boston, 2003. 183–186
12 Kaltenberger F. Relative channel reciprocity calibration in MIMO/TDD systems. In: Proceedings of IEEE Future Network and Mobile Summit, Florence, 2010. 1–10
13 Huang F, Wang Y F, Yang J, et al. Antenna mismatch and calibration problem in coordinated multi-point transmission system. IET Commun, 2012, 6: 289–299
14 Wei H. ICD reciprocity calibration for distributed large-scale MIMO systems with BD precoding. In: Proceedings of IEEE International Conference on Communications in China (ICCC), Shenzhen, 2015. 1–5
15 Huawei. Hardware calibration requirement for dual layer beamforming. In: 3GPP TSG RAN WG1 Meeting #57, R1-092359, Los Angeles, 2009. 1–10
16 Ericsson. On the need for UE calibration for enhanced downlink transmission. In: 3GPP TSG RAN WG1 Meeting #57, R1-092016, San Francisco, 2009. 1–4
17 Alcatel-Lucent. Channel reciprocity modeling and performance evaluation. In: 3GPP TSG RAN WG1 Meeting #59, R1-100426, Jeju, 2010. 1–10
18 Wang D M, Wang J Z, You X H, et al. Spectral efficiency of distributed MIMO systems. IEEE J Sel Area Commun, 2013, 31: 2112–2127
19 Wang J Z, Zhu H L, Gomes N. Distributed antenna systems for mobile communications in high speed trains. IEEE J Sel Area Commun, 2012, 30: 675–683
20 Geng J. Antenna gain mismatch calibration for cooperative base stations. In: Proceedings of IEEE Vehicular Technology Conference (VTC-Fall), San Francisco, 2011. 1–5
21 Maiwald D, Kraus D. Calculation of moments of complex wishart and complex inverse wishart distributed matrices. IEE Proc-Radar Sonar Navig, 2000, 147: 162–168
22 Zhang Q T, Cui X W, Li X M. Very tight capacity bounds for MIMO-correlated rayleigh-fading channels. IEEE Trans Wirel Commun, 2005, 4: 681–688
23 Xing C W, Ma S D, Zhou Y Q. Matrix-monotonic optimization for MIMO systems. IEEE Trans Signal Process, 2015, 63: 334–348
24 Shepard C. Argos: practical many-antenna base stations. In: Proceedings of the 18th Annual International Conference on Mobile Computing and Networking, Istanbul, 2012. 53–64
25 Wei H, Wang D M, Zhu H L, et al. Mutual coupling calibration for multiuser massive MIMO systems. IEEE Trans Wirel Commun, 2015, doi: 10.1109/TWC.2015.2476467, in press. http://ieeexplore.ieee.org/xpls/abs_all.jsp?arnumber=7239634

Appendix A Proof of Theorem 1

According to (36), by moving the ith row to the top, we transform $\boldsymbol{H}_{ii}^{\tau}$ into

$$\boldsymbol{H}_{ii\_\text{reform}}^{\tau} = \begin{bmatrix} h_{i1}\tau_1 & \cdots & h_{im}\tau_m & \cdots & h_{iM}\tau_M \\ h_{11} & \cdots & h_{1m} & \cdots & h_{1M} \\ \vdots & & \vdots & & \vdots \\ h_{(i-1)1} & \cdots & h_{(i-1)m} & \cdots & h_{(i-1)M} \\ h_{(i+1)1} & \cdots & h_{(i+1)m} & \cdots & h_{(i+1)M} \\ \vdots & & \vdots & & \vdots \\ h_{K1} & \cdots & h_{Km} & \cdots & h_{KM} \end{bmatrix}. \tag{A1}$$

Then, we write $\boldsymbol{H}_{ii\_\mathrm{reform}}^{\tau}$ as $\boldsymbol{H}_{ii\_\mathrm{reform}}^{\tau}=[\,\boldsymbol{a}_i^{\tau\mathrm{T}}\ \ \boldsymbol{A}_{\overline{i}}^{\mathrm{T}}\,]^{\mathrm{T}}$, where

$$\boldsymbol{a}_i^{\tau}=[h_{i1}\tau_1,\dots h_{im}\tau_m,\dots h_{iM}\tau_M],\quad \boldsymbol{A}_{\overline{i}}=\begin{bmatrix} h_{11} & \cdots & h_{1m} & \cdots & h_{1M}\\ \vdots & & \vdots & & \vdots\\ h_{(i-1)1} & \cdots & h_{(i-1)m} & \cdots & h_{(i-1)M}\\ h_{(i+1)1} & \cdots & h_{(i+1)m} & \cdots & h_{(i+1)M}\\ \vdots & & \vdots & & \vdots\\ h_{K1} & \cdots & h_{Km} & \cdots & h_{KM}\end{bmatrix}.$$

Correspondingly, we transform $\boldsymbol{H}$ into

$$\boldsymbol{H}_{i\_\mathrm{reform}}=\begin{bmatrix} h_{i1} & \cdots & h_{im} & \cdots & h_{iM}\\ h_{11} & \cdots & h_{1m} & \cdots & h_{1M}\\ \vdots & & \vdots & & \vdots\\ h_{(i-1)1} & \cdots & h_{(i-1)m} & \cdots & h_{(i-1)M}\\ h_{(i+1)1} & \cdots & h_{(i+1)m} & \cdots & h_{(i+1)M}\\ \vdots & & \vdots & & \vdots\\ h_{K1} & \cdots & h_{Km} & \cdots & h_{KM}\end{bmatrix},\tag{A2}$$

and write $\boldsymbol{H}_{i\_\mathrm{reform}}$ as $\boldsymbol{H}_{i\_\mathrm{reform}}^{\tau}=[\,\boldsymbol{a}_i^{\mathrm{T}}\ \ \boldsymbol{A}_{\overline{i}}^{\mathrm{T}}\,]^{\mathrm{T}}$, where $\boldsymbol{a}_i=[h_{i1},\dots h_{im},\dots h_{iM}]$. Define

$$\boldsymbol{\Phi}_{ii}^{\tau}=\boldsymbol{H}_{ii\_\mathrm{reform}}^{\tau}\boldsymbol{C}_{\mathrm{BS,r}}\boldsymbol{C}_{\mathrm{BS,r}}^{*}\boldsymbol{H}^{\mathrm{H}},\quad \boldsymbol{\Phi}_i=\boldsymbol{H}_{i\_\mathrm{reform}}\boldsymbol{C}_{\mathrm{BS,r}}\boldsymbol{C}_{\mathrm{BS,r}}^{*}\boldsymbol{H}^{\mathrm{H}},\tag{A3}$$

then, according to (37) and the characteristic of the determinant, one obtains

$$\left|[\boldsymbol{W}]_{ii}\right|^2=\frac{\det\left(\boldsymbol{\Phi}_{ii}^{\tau}\boldsymbol{\Phi}_{ii}^{\tau\mathrm{H}}\right)}{\det\left(\boldsymbol{\Phi}_i\boldsymbol{\Phi}_i^{\mathrm{H}}\right)}.\tag{A4}$$

Further, according to the properties of block matrices, we have

$$\det\left(\boldsymbol{\Phi}_{ii}^{\tau}\boldsymbol{\Phi}_{ii}^{\tau\mathrm{H}}\right)=\det\left(\begin{bmatrix} u_{ii}^{\tau} & \boldsymbol{u}_{i\overline{i}}^{\tau}\\ \boldsymbol{u}_{i\overline{i}}^{\tau\mathrm{H}} & \boldsymbol{U}_{\overline{ii}}\end{bmatrix}\right)=\det\left(\boldsymbol{U}_{\overline{ii}}\right)\cdot\det\left(u_{ii}^{\tau}-\boldsymbol{u}_{i\overline{i}}^{\tau}\boldsymbol{U}_{\overline{ii}}^{-1}\boldsymbol{u}_{i\overline{i}}^{\tau\mathrm{H}}\right),\tag{A5}$$

where

$$u_{ii}^{\tau}=\boldsymbol{\psi}_i^{\tau}\boldsymbol{\psi}_i^{\tau\mathrm{H}},\quad \boldsymbol{u}_{i\overline{i}}^{\tau}=\boldsymbol{\psi}_i^{\tau}\boldsymbol{\Psi}_{\overline{i}}^{\mathrm{H}},\quad \boldsymbol{U}_{\overline{ii}}=\boldsymbol{\Psi}_{\overline{i}}\boldsymbol{\Psi}_{\overline{i}}^{\mathrm{H}},$$

and

$$\boldsymbol{\psi}_i^{\tau}=\boldsymbol{a}_i^{\tau}\boldsymbol{C}_{\mathrm{BS,r}}\boldsymbol{C}_{\mathrm{BS,r}}^{*}\boldsymbol{H}^{\mathrm{H}},\quad \boldsymbol{\Psi}_{\overline{i}}=\boldsymbol{A}_{\overline{i}}\boldsymbol{C}_{\mathrm{BS,r}}\boldsymbol{C}_{\mathrm{BS,r}}^{*}\boldsymbol{H}^{\mathrm{H}}.$$

When the number of BS antennas is large, i.e. $M\to\infty$, we can get the simple approximations as follow

$$\lim_{M\to\infty}\frac{1}{M}\cdot\sum_{j=1}^{M}|h_{ij}|^2\left|r_{\mathrm{BS},j}\right|^2=\mathcal{E}\left[\left|r_{\mathrm{BS},j}\right|^2\right]=e^{2\delta_{\mathrm{BS,r}}^2},\quad \lim_{M\to\infty}\frac{1}{M}\cdot\sum_{j=1}^{M}h_{ij}h_{kj}^{*}\left|r_{\mathrm{BS},j}\right|^2=0.\tag{A6}$$

Thus, the approximation of $\boldsymbol{\Psi}_{\overline{i}}$ is given by

$$\lim_{M\to\infty}\frac{1}{M}\cdot\left[\boldsymbol{\Psi}_{\overline{i}}\right]_{s,v}=\begin{cases} e^{2\delta_{\mathrm{BS,r}}^2}, & s=v,s\leqslant i-1,\\ e^{2\delta_{\mathrm{BS,r}}^2}, & s+1=v,\ s\geqslant i,\\ 0, & \text{others},\end{cases}\tag{A7}$$

and

$$\lim_{M\to\infty}\left[\boldsymbol{\Psi}_{\overline{i}}^{\mathrm{H}}\left(\boldsymbol{\Psi}_{\overline{i}}\boldsymbol{\Psi}_{\overline{i}}^{\mathrm{H}}\right)^{-1}\boldsymbol{\Psi}_{\overline{i}}\right]_{s,v}=\boldsymbol{I}_i^{(0)}.\tag{A8}$$

For simplicity of discussion, we defining the matrices as follow

$$\left[\boldsymbol{I}_i^{(0)}\right]_{s,v}=\begin{cases} 1, & s=v\neq i,\\ 0, & \text{others};\end{cases}\quad \left[\boldsymbol{I}_i^{(1)}\right]_{s,v}=\begin{cases} 1, & s=v=i,\\ 0, & \text{others}.\end{cases}\tag{A9}$$

Therefore, according to (A8), we obtain

$$u_{ii}^{\tau}-\boldsymbol{u}_{i\overline{i}}^{\tau}\boldsymbol{U}_{\overline{ii}}^{-1}\boldsymbol{u}_{i\overline{i}}^{\tau\mathrm{H}}=\boldsymbol{\psi}_i^{\tau}\boldsymbol{\psi}_i^{\tau\mathrm{H}}-\boldsymbol{\psi}_i^{\tau}\left[\boldsymbol{\Psi}_{\overline{i}}^{\mathrm{H}}\left(\boldsymbol{\Psi}_{\overline{i}}\boldsymbol{\Psi}_{\overline{i}}^{\mathrm{H}}\right)^{-1}\boldsymbol{\Psi}_{\overline{i}}\right]\boldsymbol{\psi}_i^{\tau\mathrm{H}}=\boldsymbol{\psi}_i^{\tau}\boldsymbol{I}_i^{(1)}\boldsymbol{\psi}_i^{\tau\mathrm{H}}=\left(\sum_{j=1}^{M}|h_{ij}|^2t_{\mathrm{BS},j}r_{\mathrm{BS},j}^{*}\right)^2.\tag{A10}$$

Since

$$\lim_{M\to\infty}\frac{1}{M}\cdot\sum_{j=1}^{M}|h_{ij}|^2 t_{\mathrm{BS},j}r^*_{\mathrm{BS},j}=\mathcal{E}\left[t_{\mathrm{BS},j}r^*_{\mathrm{BS},j}\right]=e^{\delta^2_{\mathrm{BS,t}}/2+\delta^2_{\mathrm{BS,r}}/2}\cdot\mathrm{sinc}\left(\theta_{\mathrm{BS,t}}\right)\cdot\mathrm{sinc}\left(\theta_{\mathrm{BS,r}}\right), \tag{A11}$$

then,

$$\det\left(u^{\tau}_{ii}-\boldsymbol{u}^{\tau}_{i\bar{i}}\boldsymbol{U}^{-1}_{\bar{i}\bar{i}}\boldsymbol{u}^{\tau\,\mathrm{H}}_{i\bar{i}}\right)=M^2\cdot e^{\delta^2_{\mathrm{BS,t}}+\delta^2_{\mathrm{BS,r}}}\cdot\mathrm{sinc}^2\left(\theta_{\mathrm{BS,t}}\right)\cdot\mathrm{sinc}^2\left(\theta_{\mathrm{BS,r}}\right). \tag{A12}$$

Similar with (A5),

$$\det\left(\boldsymbol{\Phi}_i\boldsymbol{\Phi}_i^{\mathrm{H}}\right)=\det\left(\begin{bmatrix}u_{ii} & \boldsymbol{u}_{i\bar{i}}\\ \boldsymbol{u}^{\mathrm{H}}_{i\bar{i}} & \boldsymbol{U}_{\bar{i}\bar{i}}\end{bmatrix}\right)=\det\left(\boldsymbol{U}_{\bar{i}\bar{i}}\right)\cdot\det\left(u_{ii}-\boldsymbol{u}_{i\bar{i}}\boldsymbol{U}^{-1}_{\bar{i}\bar{i}}\boldsymbol{u}^{\mathrm{H}}_{i\bar{i}}\right), \tag{A13}$$

where $u_{ii}=\boldsymbol{\psi}_i\boldsymbol{\psi}_i^{\mathrm{H}}$, $\boldsymbol{u}_{i\bar{i}}=\boldsymbol{\psi}_i\boldsymbol{\Psi}^{\mathrm{H}}_{\bar{i}}$, and $\boldsymbol{\psi}_i=\boldsymbol{a}_i\boldsymbol{C}_{\mathrm{BS,r}}\boldsymbol{C}^*_{\mathrm{BS,r}}\boldsymbol{H}^{\mathrm{H}}$. Consequently, we have

$$u_{ii}-\boldsymbol{u}_{i\bar{i}}\boldsymbol{U}^{-1}_{\bar{i}\bar{i}}\boldsymbol{u}^{\mathrm{H}}_{i\bar{i}}=\boldsymbol{\psi}_i\boldsymbol{\psi}_i^{\mathrm{H}}-\boldsymbol{\psi}_i\left[\boldsymbol{\Psi}^{\mathrm{H}}_{\bar{i}}\left(\boldsymbol{\Psi}_{\bar{i}}\boldsymbol{\Psi}^{\mathrm{H}}_{\bar{i}}\right)^{-1}\boldsymbol{\Psi}_{\bar{i}}\right]\boldsymbol{\psi}_i^{\mathrm{H}}=\boldsymbol{\psi}_i\boldsymbol{I}_i^{(1)}\boldsymbol{\psi}_i^{\mathrm{H}}=\left(\sum_{j=1}^{M}|h_{ij}|^2|r_{\mathrm{BS},j}|^2\right)^2. \tag{A14}$$

Then, according to (A6), one obtains

$$\det\left(u_{ii}-\boldsymbol{u}_{i\bar{i}}\boldsymbol{U}^{-1}_{\bar{i}\bar{i}}\boldsymbol{u}^{\mathrm{H}}_{i\bar{i}}\right)=M^2\cdot e^{4\delta^2_{\mathrm{BS,r}}}. \tag{A15}$$

By the approximations above, we can derive the simple close-form expression of $\left|[\boldsymbol{W}]_{ii}\right|^2$ as

$$\begin{aligned}\left|[\boldsymbol{W}]_{ii}\right|^2&=\frac{\det\left(\boldsymbol{U}_{\bar{i}\bar{i}}\right)\cdot\det\left(u^{\tau}_{ii}-\boldsymbol{u}^{\tau}_{i\bar{i}}\boldsymbol{U}^{-1}_{\bar{i}\bar{i}}\boldsymbol{u}^{\tau\,\mathrm{H}}_{i\bar{i}}\right)}{\det\left(\boldsymbol{U}_{\bar{i}\bar{i}}\right)\cdot\det\left(u_{ii}-\boldsymbol{u}_{i\bar{i}}\boldsymbol{U}^{-1}_{\bar{i}\bar{i}}\boldsymbol{u}^{\mathrm{H}}_{i\bar{i}}\right)}=\frac{\det\left(u^{\tau}_{ii}-\boldsymbol{u}^{\tau}_{i\bar{i}}\boldsymbol{U}^{-1}_{\bar{i}\bar{i}}\boldsymbol{u}^{\tau\,\mathrm{H}}_{i\bar{i}}\right)}{\det\left(u_{ii}-\boldsymbol{u}_{i\bar{i}}\boldsymbol{U}^{-1}_{\bar{i}\bar{i}}\boldsymbol{u}^{\mathrm{H}}_{i\bar{i}}\right)}\\&=\frac{e^{\delta^2_{\mathrm{BS,t}}+\delta^2_{\mathrm{BS,r}}}\cdot\mathrm{sinc}^2\left(\theta_{\mathrm{BS,t}}\right)\cdot\mathrm{sinc}^2\left(\theta_{\mathrm{BS,r}}\right)}{e^{4\delta^2_{\mathrm{BS,r}}}}.\end{aligned} \tag{A16}$$

Appendix B Proof of Theorem 2

According to (39), by subtracting the ith row from the jth row and moving the jth row to the top, we transform $\boldsymbol{H}_{ij}$ into

$$\boldsymbol{H}^{\tau 1}_{ij\_\mathrm{reform}}=\begin{bmatrix}h_{i1}\left(\tau_1-1\right) & \cdots & h_{im}\left(\tau_m-1\right) & \cdots & h_{iM}\left(\tau_M-1\right)\\ h_{11} & \cdots & h_{1m} & \cdots & h_{1M}\\ \vdots & & \vdots & & \vdots\\ h_{i1} & \cdots & h_{im} & \cdots & h_{iM}\\ \vdots & & \vdots & & \vdots\\ h_{(j-1)1} & \cdots & h_{(j-1)m} & \cdots & h_{(j-1)M}\\ h_{(j+1)1} & \cdots & h_{(j+1)m} & \cdots & h_{(j+1)M}\\ \vdots & & \vdots & & \vdots\\ h_{K1} & \cdots & h_{Km} & \cdots & h_{KM}\end{bmatrix}. \tag{B1}$$

Then, we write $\boldsymbol{H}^{\tau 1}_{ij\_\mathrm{reform}}$ as $\boldsymbol{H}^{\tau 1}_{ij\_\mathrm{reform}}=[\,\boldsymbol{a}_i^{\tau 1\,\mathrm{T}}\;\;\boldsymbol{A}^{\mathrm{T}}_{\bar{j}}\,]^{\mathrm{T}}$, where

$$\boldsymbol{a}_i^{\tau 1}=\left[h_{i1}\left(\tau_1-1\right),\ldots h_{im}\left(\tau_m-1\right),\ldots h_{iM}\left(\tau_M-1\right)\right].$$

Correspondingly, we transform $\boldsymbol{H}$ into

$$\boldsymbol{H}_{j\_\mathrm{reform}}=\begin{bmatrix}h_{j1} & \cdots & h_{jm} & \cdots & h_{jM}\\ h_{11} & \cdots & h_{1m} & \cdots & h_{1M}\\ \vdots & & \vdots & & \vdots\\ h_{(j-1)1} & \cdots & h_{(j-1)m} & \cdots & h_{(j-1)M}\\ h_{(j+1)1} & \cdots & h_{(j+1)m} & \cdots & h_{(j+1)M}\\ \vdots & & \vdots & & \vdots\\ h_{K1} & \cdots & h_{Km} & \cdots & h_{KM}\end{bmatrix}, \tag{B2}$$

and write $\boldsymbol{H}_{j\_\mathrm{reform}}$ as $\boldsymbol{H}_{j\_\mathrm{reform}}=[\,\boldsymbol{a}_j^{\mathrm{T}}\;\;\boldsymbol{A}^{\mathrm{T}}_{\bar{j}}\,]^{\mathrm{T}}$, where

$$\boldsymbol{a}_j=\left[h_{j1},\ldots h_{jm},\ldots h_{jM}\right].$$

Define

$$\boldsymbol{\Phi}^{\tau 1}_{ij}=\boldsymbol{H}^{\tau 1}_{ij\_\mathrm{reform}}\boldsymbol{C}_{\mathrm{BS,r}}\boldsymbol{C}^*_{\mathrm{BS,r}}\boldsymbol{H}^{\mathrm{H}},\quad\boldsymbol{\Phi}_j=\boldsymbol{H}_{j\_\mathrm{reform}}\boldsymbol{C}_{\mathrm{BS,r}}\boldsymbol{C}^*_{\mathrm{BS,r}}\boldsymbol{H}^{\mathrm{H}}, \tag{B3}$$

then, according to (40) and the characteristic of the determinant, one obtains

$$\left|[\boldsymbol{W}]_{ij}\right|^2 = \frac{\det\left(\boldsymbol{\Phi}_{ij}^{\tau 1}\boldsymbol{\Phi}_{ij}^{\tau 1\mathrm{H}}\right)}{\det\left(\boldsymbol{\Phi}_j\boldsymbol{\Phi}_j^{\mathrm{H}}\right)}. \tag{B4}$$

Further, according to the properties of block matrices, we have

$$\det\left(\boldsymbol{\Phi}_{ij}^{\tau 1}\boldsymbol{\Phi}_{ij}^{\tau 1\mathrm{H}}\right) = \det\left(\begin{bmatrix} u_{ii}^{\tau 1} & \boldsymbol{u}_{i\overline{j}}^{\tau 1} \\ \boldsymbol{u}_{i\overline{j}}^{\tau 1\mathrm{H}} & \boldsymbol{U}_{\overline{jj}} \end{bmatrix}\right) = \det\left(\boldsymbol{U}_{\overline{jj}}\right)\cdot\det\left(u_{ii}^{\tau 1} - \boldsymbol{u}_{i\overline{j}}^{\tau 1}\boldsymbol{U}_{\overline{jj}}^{-1}\boldsymbol{u}_{i\overline{j}}^{\tau 1\mathrm{H}}\right), \tag{B5}$$

where

$$u_{ii}^{\tau 1} = \boldsymbol{\psi}_i^{\tau 1}\boldsymbol{\psi}_i^{\tau 1\mathrm{H}}, \quad \boldsymbol{u}_{i\overline{j}}^{\tau 1} = \boldsymbol{\psi}_i^{\tau 1}\boldsymbol{\Psi}_{\overline{j}}^{\mathrm{H}}, \boldsymbol{U}_{\overline{jj}} = \boldsymbol{\Psi}_{\overline{j}}\boldsymbol{\Psi}_{\overline{j}}^{\mathrm{H}},$$

and

$$\boldsymbol{\psi}_i^{\tau} = \boldsymbol{a}_i^{\tau 1}\boldsymbol{C}_{\mathrm{BS,r}}\boldsymbol{C}_{\mathrm{BS,r}}^{*}\boldsymbol{H}^{\mathrm{H}}, \quad \boldsymbol{\Psi}_{\overline{j}} = \boldsymbol{A}_{\overline{j}}\boldsymbol{C}_{\mathrm{BS,r}}\boldsymbol{C}_{\mathrm{BS,r}}^{*}\boldsymbol{H}^{\mathrm{H}}.$$

Similar with (A8), we can get the get the approximation as follows

$$\lim_{M\to\infty}\left[\boldsymbol{\Psi}_{\overline{j}}^{\mathrm{H}}\left(\boldsymbol{\Psi}_{\overline{j}}\boldsymbol{\Psi}_{\overline{j}}^{\mathrm{H}}\right)^{-1}\boldsymbol{\Psi}_{\overline{j}}\right]_{s,v} = \boldsymbol{I}_j^{(0)}. \tag{B6}$$

Therefore, we obtain

$$\begin{aligned} u_{ii}^{\tau 1} - \boldsymbol{u}_{i\overline{j}}^{\tau 1}\boldsymbol{U}_{\overline{jj}}^{-1}\boldsymbol{u}_{i\overline{j}}^{\tau 1\mathrm{H}} &= \boldsymbol{\psi}_i^{\tau 1}\boldsymbol{\psi}_i^{\tau 1\mathrm{H}} - \boldsymbol{\psi}_i^{\tau 1}\left[\boldsymbol{\Psi}_{\overline{j}}^{\mathrm{H}}\left(\boldsymbol{\Psi}_{\overline{j}}\boldsymbol{\Psi}_{\overline{j}}^{\mathrm{H}}\right)^{-1}\boldsymbol{\Psi}_{\overline{j}}\right]\boldsymbol{\psi}_i^{\tau 1\mathrm{H}} = \boldsymbol{\psi}_i^{\tau 1}\boldsymbol{I}_j^{(1)}\boldsymbol{\psi}_i^{\tau 1\mathrm{H}} \\ &= \left|\sum_{k=1}^{M} h_{ik}h_{jk}^{*}\left(t_{\mathrm{BS},k} - r_{\mathrm{BS},k}^{*}\right)r_{\mathrm{BS},k}\right|^2. \end{aligned} \tag{B7}$$

Since

$$\begin{aligned} &\lim_{M\to\infty}\frac{1}{M}\cdot\left|\sum_{k=1}^{M} h_{ik}h_{jk}^{*}\left(t_{\mathrm{BS},k} - r_{\mathrm{BS},k}\right)r_{\mathrm{BS},k}^{*}\right|^2 \\ &= \mathcal{E}\left[\left|t_{\mathrm{BS},k}\right|^2 + \left|r_{\mathrm{BS},k}\right|^2 - 2t_{\mathrm{BS},k}r_{\mathrm{BS},k}\right]\cdot\mathcal{E}\left[\left|r_{\mathrm{BS},k}\right|^2\right] \\ &= e^{2\delta_{\mathrm{BS,r}}^2}\cdot\left[e^{2\delta_{\mathrm{BS,t}}^2} + e^{2\delta_{\mathrm{BS,r}}^2} - 2e^{\delta_{\mathrm{BS,t}}^2/2 + \delta_{\mathrm{BS,r}}^2/2}\cdot\mathrm{sinc}\left(\theta_{\mathrm{BS,t}}\right)\cdot\mathrm{sinc}\left(\theta_{\mathrm{BS,r}}\right)\right], \end{aligned} \tag{B8}$$

then,

$$\det\left(u_{ii}^{\tau 1} - \boldsymbol{u}_{i\overline{j}}^{\tau 1}\boldsymbol{U}_{\overline{jj}}^{-1}\boldsymbol{u}_{i\overline{j}}^{\tau 1\mathrm{H}}\right) = M\cdot e^{2\delta_{\mathrm{BS,r}}^2}\cdot\left[e^{2\delta_{\mathrm{BS,t}}^2} + e^{2\delta_{\mathrm{BS,r}}^2} - 2e^{\delta_{\mathrm{BS,t}}^2/2 + \delta_{\mathrm{BS,r}}^2/2}\cdot\mathrm{sinc}\left(\theta_{\mathrm{BS,t}}\right)\cdot\mathrm{sinc}\left(\theta_{\mathrm{BS,r}}\right)\right]. \tag{B9}$$

Similar with (A13)–(A15), we obtain

$$\det\left(\boldsymbol{\Phi}_j\boldsymbol{\Phi}_j^{\mathrm{H}}\right) = \det\left(\begin{bmatrix} u_{jj} & \boldsymbol{u}_{j\overline{j}} \\ \boldsymbol{u}_{j\overline{j}}^{\mathrm{H}} & \boldsymbol{U}_{\overline{jj}} \end{bmatrix}\right) = \det\left(\boldsymbol{U}_{\overline{jj}}\right)\cdot\det\left(u_{jj} - \boldsymbol{u}_{j\overline{j}}\boldsymbol{U}_{\overline{jj}}^{-1}\boldsymbol{u}_{j\overline{j}}^{\mathrm{H}}\right), \tag{B10}$$

and

$$\det\left(u_{jj} - \boldsymbol{u}_{j\overline{j}}\boldsymbol{U}_{\overline{jj}}^{-1}\boldsymbol{u}_{j\overline{j}}^{\mathrm{H}}\right) = M^2\cdot e^{4\delta_{\mathrm{BS,r}}^2}. \tag{B11}$$

Therefore, we can derive the simple close-form expression of $|[\boldsymbol{W}]_{ij}|^2$ as

$$\begin{aligned} \left|[\boldsymbol{W}]_{ij}\right|^2 &= \frac{\det\left(\boldsymbol{U}_{\overline{jj}}\right)\cdot\det\left(u_{ii}^{\tau 1} - \boldsymbol{u}_{i\overline{j}}^{\tau 1}\boldsymbol{U}_{\overline{ij}}^{-1}\boldsymbol{u}_{i\overline{j}}^{\tau 1\mathrm{H}}\right)}{\det\left(\boldsymbol{U}_{\overline{jj}}\right)\cdot\det\left(u_{jj} - \boldsymbol{u}_{j\overline{j}}\boldsymbol{U}_{\overline{jj}}^{-1}\boldsymbol{u}_{j\overline{j}}^{\mathrm{H}}\right)} \\ &= \frac{\det\left(u_{ii}^{\tau 1} - \boldsymbol{u}_{i\overline{j}}^{\tau 1}\boldsymbol{U}_{\overline{jj}}^{-1}\boldsymbol{u}_{i\overline{j}}^{\tau 1\mathrm{H}}\right)}{\det\left(u_{jj} - \boldsymbol{u}_{j\overline{j}}\boldsymbol{U}_{\overline{jj}}^{-1}\boldsymbol{u}_{j\overline{j}}^{\mathrm{H}}\right)} \\ &= \frac{1}{M}\cdot\frac{1}{e^{2\delta_{\mathrm{BS,r}}^2}}\cdot\left[e^{2\delta_{\mathrm{BS,t}}^2} + e^{2\delta_{\mathrm{BS,r}}^2} - 2e^{\delta_{\mathrm{BS,t}}^2/2 + \delta_{\mathrm{BS,r}}^2/2}\cdot\mathrm{sinc}\left(\theta_{\mathrm{BS,t}}\right)\cdot\mathrm{sinc}\left(\theta_{\mathrm{BS,r}}\right)\right]. \end{aligned} \tag{B12}$$